Extending the Benchmark Cable-Stayed Bridge for Transverse Response under Seismic Loading

M. Domaneschi, Ph.D.[1]; and L. Martinelli, Ph.D.[2]

Introduction

The scientific community recognizes benchmarking as a fruitful research exercise in many fields. In structural control, it results in the development of more suitable models for comparing different solutions, exploiting new technologies, and analyzing original behaviors. The most attractive outcomes are usually selected by means of evaluation criteria defined in the benchmark statement (e.g., Dyke et al. 2003; Caicedo et al. 2003).

The benchmark on the Bill Emerson cable-stayed bridge has attracted the attention of many specialists in the field of structural control and dynamics from its starting Phase I version (Dyke et al. 2003). In its latest Phase II (Caicedo et al. 2003), the benchmark was extended to analyze the bidirectional behavior of the cable-stayed bridge, implementing orthogonal horizontal seismic motion components. Moreover, in Phase II, evaluation criteria in the transversal direction are introduced that complement those in the longitudinal direction of Phase I.

Several papers have contributed to the benchmark Phase II up to very recently. The first to be mentioned is the original statement (Caicedo et al. 2003), in which an active control solution is presented as the best compromise between the internal actions of the bridge and displacement reduction. Park et al. (2003) studied hybrid control systems composed of passive devices to reduce the internal forces and active (or semiactive) ones to further reduce the deck displacements in the longitudinal direction. Loh and Chang (2006) have implemented semiactive magnetorheological (MR) dampers to compare several control laws. He and Agrawal (2007) investigated a hybrid control strategy (passive and semiactive devices) on the bridge model by a large number of recorded near-field ground motions. Domaneschi (2010) proposed passive and semiactive decentralized schemes with good robustness qualities that are able to perform similarly to the active ones proposed in the original statement. More recently, Fallah and Taghikhany (2011) reported on an effective decentralized control system, focusing attention on time delay in the feedback.

All these control applications mitigate the longitudinal seismic response of the cable-stayed bridge using a variety of control techniques, highlighting the importance of the benchmark problem and improving on the knowledge. However, the structural responses in the transversal direction in terms of internal actions and displacements are either not mitigated or disregarded right away in the literature because they change insignificantly.

In light of these observations, this paper enriches the literature on the benchmark Phase II by achieving a substantial mitigation of the seismic transversal response for the case in study without losing focus on the mitigation of the longitudinal response. This has been possible from the original *MATLAB* model given as part of Phases I and II of the benchmark, developing a new improved bridge model.

Since the original benchmark disregarded possible soil-structure interaction (SSI), to offer an improved view, the new bridge numerical model developed in this paper introduces SSI through the use of impedance functions and the foundations were assumed at the bedrock (Wilson and Gravelle 1991). The improved bridge model adopts the finite-element (FE) discretization recently presented for a performance comparison of passive control strategies (Domaneschi and Martinelli 2012). Apart from the simulation improvements in the cable dynamics in the SSI and considering geometric nonlinearities, as reported in details in a specific section of this work, the new model allows for removal of the deck transversal rigid links implemented in the original benchmark. This permits the evaluation of the role they play in the efficiency of the control system. In fact, one of the goals of this work consisted of reducing the evaluation criteria linked to the transversal direction, either for the internal actions or the displacements, which

[1]Contract Professor of Structural Mechanics, Dept. of Civil and Environmental Engineering, Politecnico di Milano, P.zza Leonardo da Vinci 32, 20133 Milano, Italy (corresponding author). E-mail: marco.domaneschi@polimi.it

[2]Assistant Professor, Dept. of Civil and Environmental Engineering, Politecnico di Milano, P.zza Leonardo da Vinci 32, 20133 Milano, Italy. E-mail: luca.martinelli@polimi.it

have never been mitigated before in the literature, starting from the control example of the original statement (Caicedo et al. 2003).

The impact of the transversal deck displacements is assessed for a set of passive and semiactive control strategies that have already been proven effective in a preceding work on the original benchmark (Domaneschi 2010). For the semiactive strategy, a decentralized scheme has been developed with the aim of breaking down the centralized approach into a number of simpler subsystems. A low order collocated control algorithm manages each control device on the base of the collected monitoring data (Preumont 2002; Frangopol et al. 2012). This solution, in particular, is suitable to answer the requirements of new research tendencies and to achieve a highly efficient control, integrated with monitoring, by producing large control forces with a small energy supply (Ikeda 2009).

Bridge Structure and Numerical Model

The bridge structure object of the control benchmark (Caicedo et al. 2003) is a fan-type cable-stayed bridge [Podolny 1980; University Transportation Center at the University of Missouri-Rolla (UTC-UMR) 2007] spanning the Mississippi River near Cape Girardeau in the United States (Fig. 1). The updated, with respect to the benchmark statement, numerical model of the bridge is developed in the *ANSYS* framework (ANSYS 2011) and comprises 3,336 degrees of freedom (DOFs) and 1,578 elements. The bridge deck has been simulated by shell elements for the concrete slab supported by a plane frame of steel beams. A short summary of the improvements will be listed in the following.

The first improved aspect pertains to SSI; this is implemented through the use of impedance functions (Sieffert and Cevaer 1992) at the foundations. The foundation is simulated by lumped masses with equivalent spring and dampers. Additional details will be given in a following section. Domaneschi and Martinelli (2012) and Ismail et al. (2013) provide a more detailed exposition.

A second aspect that has been improved is modeling of the stays. The original benchmark statement does not consider DOFs for the cables beside those of the extreme nodes, neglecting the description of their dynamics and interactions with the bridge so that only the bridge deck motion is accounted for (Caicedo et al. 2003). This approach, also called *one-element cable system* and proposed in its latest version by Wilson and Gravelle (1991), is a practical solution with several applications. However, the modeling of the stay cables needs special care and can be highly improved (Caetano et al. 2008). Focusing attention on this aspect, each cable has been modeled with six tension-only truss elements for each cable. This number of elements is sufficiently large to give rise to small errors (Gattulli and Lepidi 2007), and is sufficient to highlight a significant variation in the cable-related evaluation criteria without overly increasing the size of the numerical problem.

One of the factors contributing to the dynamic behavior of a flexible structure, like a cable-stayed bridge, is the nonlinear relation
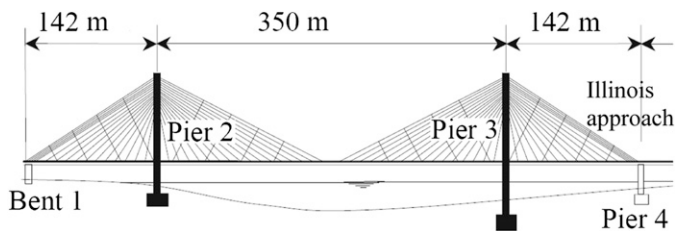
Fig. 1. Bridge geometry scheme

between deformations and displacements (Chen and Duan 2000) in the form of geometric nonlinearities or second-order effects. In the improved bridge model, such a dependency is accounted for by evaluating the dynamic equilibrium of the structure in the deformed configuration at each time instant.

Multiple-Support Input and Soil-Structure Interaction

The original benchmark considered multiple-support excitation by applying the same ground motion at each support with a time delay due to the finite velocity of propagation of the seismic waves. In the updated model, the equations of motion of the soil-structure system subjected to multiple-support seismic excitation are written in matrix form (Clough and Penzien 1975; Martinelli et al. 2010, 2011) as

$$\mathbf{M}\ddot{\mathbf{q}} + \mathbf{C}\dot{\mathbf{q}} = \mathbf{R} + \mathbf{Q}_s + \mathbf{Q} \qquad (1)$$

where $\mathbf{q}$ = vector of Lagrangian coordinates representing the total generalized displacements; $\mathbf{M}$ and $\mathbf{C}$ = inertia and damping matrices; and $\mathbf{R}$, $\mathbf{Q}_s$, and $\mathbf{Q}$ = vectors listing the generalized components of the nonlinear restoring forces of the equivalent seismic forces and the other dynamic forces, respectively. A dot denotes the derivative with respect to time.

Impedance Relations for the Bridge Foundations

The SSI is accounted for by the use of impedance functions. If linear behavior of the ground and lumped parameters (frequency independent) modeling of the SSI is assumed, the seismic term can be expressed as

$$Q_s = \begin{bmatrix} 0 \\ \mathbf{C}_{CC}^{(g)}\dot{\mathbf{q}}_C^{(f)} \end{bmatrix} + \begin{bmatrix} 0 \\ \mathbf{K}_{CC}^{(g)}\mathbf{q}_C^{(f)} \end{bmatrix} \qquad (2)$$

where $\mathbf{q}_C^{(f)}$ = vector listing the free-field ground displacement at the soil-structure contact points; and $\mathbf{C}_{CC}^{(g)}$ and $\mathbf{K}_{CC}^{(g)}$ = soil damping and stiffness matrices referred to the free-field ground velocities and displacements at the soil-structure contact points, respectively.

This corresponds to inserting linear elastic springs in the vertical z-direction, transversal y-direction, and longitudinal x-direction, respectively, for both translational and rotational DOFs at each foundation and viscous linear dashpots acting in parallel to the springs for the translational DOFs. The spring stiffness and the dashpot constant populate matrices $\mathbf{K}_{CC}^{(g)}$ and $\mathbf{C}_{CC}^{(g)}$, respectively.

Computation of the stiffness and damping constants is based upon the instructions reported by Sieffert and Cevaer (1992) under the hypotheses of a rigid circular foundation and soil modeled as an elastic semispace. In the case in the study, the foundation of the towers has a rectangular shape, so the equivalent circular one of radius r is evaluated. In particular, the following DOFs have been considered: translational, $r_{x,y,z} = (4B/\pi)^{1/2} = 17.7$ m; rocking around the longitudinal x-axis, $r_{rx} = (16B^3L/3\pi)^{1/4} = 21.5$ m; rocking around the transversal y-axis, $r_{ry} = (16BL^3/3\pi)^{1/4} = 15$ m; and torsional, $r_{tz} = [8BL(B^2 + L^2)/3\pi]^{1/4} = 19.1$ m. In these equations, B and L are the half-transversal and longitudinal dimensions for the tower foundations, respectively (Sieffert and Cevaer 1992).

The values for the elastic constants have been selected, paying attention to the bridge support foundations, and consist of piles in alluvial material. They have been chosen as a mean value between rigid and soft soil parameters to mitigate the higher pile stiffness, allowing finite deformations by the soil where the deep foundations are fixed (shear modulus $G = 10^6$ kN/m^2; $\nu = 0.33$).

Consequently, the following equivalent stiffness and damping values result: $k_z = 1.062 \times 10^8$ kN/m and $c_z = 2 \times 10^6$ kNs/m; $k_{x,y} = 8.5 \times 10^7$ kN/m and $c_{x,y} = 1.2 \times 10^6$ kNs/m; $k_{rx} = 3.97 \times 10^{10}$ kNm/rad; $k_{ry} = 1.35 \times 10^{10}$ kNm/rad; and $k_{tz} = 3.71 \times 10^{10}$ kNm/rad. It is also worth noting that such parameters also allow correct matching of the modal frequencies reported in the benchmark problem statement for the uncontrolled structural configuration.

Finally, $\mathbf{q}_C^{(f)}$ and $\dot{\mathbf{q}}_C^{(f)}$ have been gained from the seismic records (El Centro, Gebze, and Mexico City) of the original benchmark. These have been oriented with an incidence angle of 15° with the bridge main axis (Caicedo et al. 2003), aiming to be consistent with Domaneschi (2010). It has been assumed that the motion at each support is delayed based on the distance from bent 1 (see Fig. 1) and the speed of the Love waves of a typical earthquake (Clough and Penzien 1975). Fig. 2 depicts the rotated components parallel to the bridge deck (longitudinal) and transversal of the seismic records. Note that the Gebze signal, which is different from the El Centro and Mexico City signals, has significant energy content for very low frequency values.

Bridge Control Strategies

The original benchmark statement leaves the choice of the control system open. In this work, a passive control system consisting of hysteretic devices has been firstly adopted thanks to its ability to act as an internal fuse for the forces applied to the supports by the deck to dissipate a large part of the seismic energy introduced into the structural system to shift the main bridge's natural frequencies far from the most dangerous input frequencies and to supply additional damping to the bridge dynamics.

The control devices, connecting the deck with the piers, are located under the bridge deck symmetrically with respect to the longitudinal axis. Two control arrangements are considered herein:

- Arrangement 1: Eight control devices act in the longitudinal direction along the deck: two at each of the four bridge support points (see Fig. 3 for those at the pier). In the transversal direction, the relative motion of the deck piers is restrained.
- Arrangement 2: A total of 16 control devices: two longitudinal and two transversal at each support point along the bridge deck.
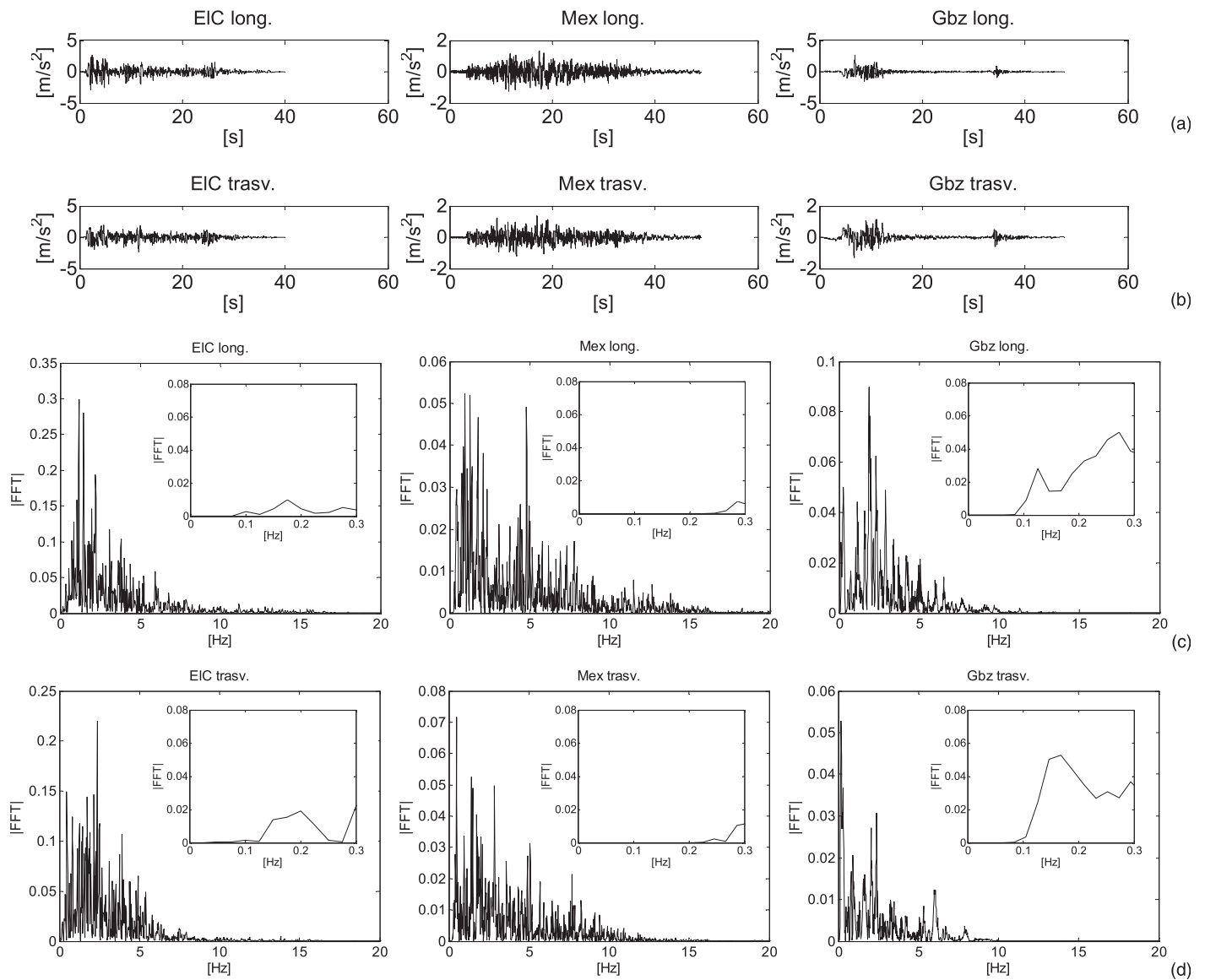
Fig. 2. El Centro, Mexico, and Gebze records: (a) longitudinal component and (b) transversal component; (c) Fourier spectra of longitudinal component and (d) transversal component with low frequencies detail

TOP VIEW

Longitudinal control device
(**for both *Arrangements 1* and *2*)

Transversal control device
(***Arrangement 2* only**)

Deck longitudinal axis

Structural connections

Section A

(DECK)

Tower transversal beam

SECTION A

Deck longitudinal axis

Transversal control device
(***Arrangement 2* only**)

Longitudinal control device
(**for both *Arrangements 1* and *2*)

(a)

Deck connection
(spherical hinge)

$x_{rel}, \dot{x}_{rel}$

Sensor $(x, \dot{x})$

Control device

Sensor $(x, \dot{x})$

Pier connection
(spherical hinge)

(b)

Fig. 3. (a) Connections under the deck at the pier support for Arrangements 1 and 2; (b) control device connection and monitoring system scheme

Fig. 3(a) shows the schematic layout of the control systems. Arrangement 1 coincides with the solution adopted by Domaneschi (2010) for the original benchmark statement, where the deck does not have a transversal relative displacement with respect to the piers. Arrangement 2 has been selected to evaluate the effectiveness of the transversal devices, which have been customarily considered in-effective in mitigating the structural response in the transversal direction in the literature (e.g., Caicedo et al. 2003; Park et al. 2003; Loh and Chang 2006; He and Agrawal 2007; Domaneschi 2010; Fallah and Taghikhany 2011). This has been possible by abandoning the original *MATLAB* model given as part of Phases I and II of the benchmark and by developing a new improved bridge model in the *ANSYS* framework.

For both Arrangements 1 and 2, the natural frequencies are at 0.12 Hz of the pure longitudinal mode, 0.19 Hz of the vertical antisymmetric model, 0.20 Hz of the torsional antisymmetric mode, and 0.24 Hz of the vertical symmetric mode, whereas the modal frequencies of the uncontrolled bridge are the same as those reported in the benchmark statement (Caicedo et al. 2003). A hysteretic behavior simulated by implementing the Bouc-Wen model in an *ANSYS* external user element, as detailed by Domaneschi et al. (2010), characterize the devices.

Semiactive Choice with Decentralization

Passive systems have the advantage of being generally more robust than active systems because they are independent from external power sources and processed commands. They sport fewer operating costs and require a lower maintenance. Their main disadvantage is their inability to adapt to different intensities of excitation. To overcome this limit, semiactive control schemes are also implemented on the refined bridge model in a decentralized configuration. The implemented semiactive control law is the on/off sky-hook one: low-order in the sense that it only uses feedback from the nodes that are directly influenced by the devices [Fig. 3(b)], and collocated
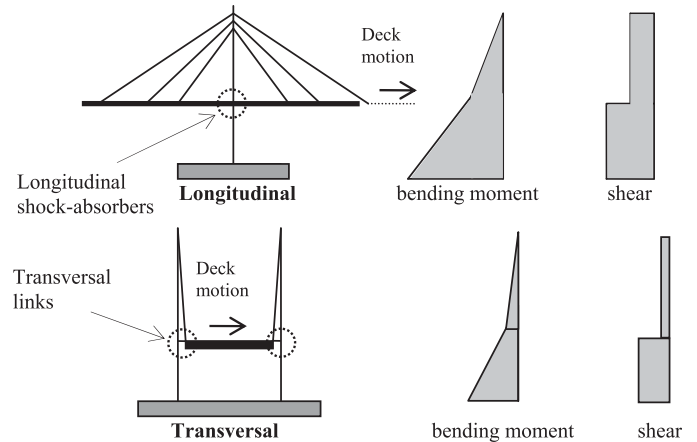
Fig. 4. Scheme of the internal forces of the pier for the uncontrolled configuration of the bridge

because the processed control forces act along the same DOF along which the monitoring data are collected. This type of control strategy enjoys the same positive qualities of passive systems, requiring only a limited amount of active external power to modify the working parameters of the semiactive control devices. This is contrary to the active control case, in which the external power is used to directly inject mechanical energy in the structure through the reactions at the device ends. Additionally, the decentralized scheme provides robustness qualities in the presence of a device failure because each device works independently from all the others (Spencer and Nagarajaiah 2003; Kelly 2004; Casciati et al. 2006; Domaneschi 2010). The selected control law has been able to adapt the device performance to the peculiarities of external excitation and to reduce the vibration amplitude between the two points on the bridge deck and on the pier/bent, respectively, where it is connected.

Implementation of the Passive and Semiactive Devices

According to the Bouc-Wen model, the equations governing the restoring force produced at each passive device end are

$$\dot{z} = A\dot{q}_{rel} - \beta \dot{q}_{rel}|z|^n - \gamma |\dot{q}_{rel}||z|z|^{n-1} \qquad (3)$$

$$\Phi(q_{rel}, t) = (1 - \alpha)Kz + \alpha K q_{rel} + c\dot{q}_{rel} \qquad (4)$$

where q_{rel} = relative displacement between the device ends; $\dot{q}_{rel}$ = relative velocity; z = auxiliary variable controlling the hysteretic behavior; Φ = device control force expressed by the sum of three terms acting in parallel; α = ratio between postyielding and preyielding stiffness; A, β, γ, and n = time-invariant parameters defining the amplitude and shape of the cycles, linearity in unloading, and smoothness of the transition from the preyield to the postyield region; K = stiffness coefficient; and c = damping coefficient. The viscous damping component is often very small, so in this formulation, it is neglected.

In the case in which $A = 1$ and α is close to zero, the yielding force Φ_y assumes the form (Casciati and Faravelli 1991; Domaneschi 2012)

$$\Phi_y = \frac{K}{(\beta + \gamma)^{1/n}} \qquad (5)$$

Such formulation is useful for the identification process of the hysteretic device.

When the semiactive property is implemented, the on/off skyhook control law is used. The choice between a high or low response level is based on the following rule:

$$\dot{q}_{deck}(\dot{q}_{deck} - \dot{q}_{tower}) \geq 0 \rightarrow \text{high} \qquad (6)$$

$$\dot{q}_{deck}(\dot{q}_{deck} - \dot{q}_{tower}) < 0 \rightarrow \text{low} \qquad (7)$$

where $\dot{q}_{deck}$ and $\dot{q}_{tower}$ = absolute velocities of the deck and the tower, respectively, at the device ends. If the product is positive or zero, the yielding force Φ_y is adjusted to its high level; otherwise, it is set to the low level (Casciati et al. 2006). This adjustment is performed by acting on the parameters β and γ. The complete formulation of the semiactive numerical model comes from Domaneschi (2012).

The device's properties are selected as reported by Fallah and Taghikhany (2011). When the passive scheme is adopted, the devices take on the following characteristics: $\Phi_y = 1,000$ kN; $K = 80,000$ kN/m; $\alpha = 0.02$; and A and n assume unitary values [device Type 1 in Domaneschi (2010)]. When the semiactive properties are implemented, the elastic limit Φ_y is fixed to 1,000 kN for the high state of the sky-hook algorithm and to 250 kN for the low state.

Results of the Time History Analyses for the Seismic Input

The bridge response is evaluated by the same peak responses as defined in the original benchmark statement (Caicedo et al. 2003).

Table 1. Arrangement 1

Seismic records	Evaluation criteria	Passive				Semiactive			
		ElC	Mex	Geb	0.3 Geb	ElC	Mex	Geb	0.3 Geb
Base shear	J1x	0.31	0.20	0.72	0.52	0.34	0.23	0.76	0.83
	J1y	1.13	1.13	1.10	0.76	1.13	1.11	1.10	1.41
Deck shear	J2x	0.57	0.56	2.73	2.43	0.57	0.57	2.63	2.71
	J2y	1.51	0.90	1.18	1.04	1.51	0.90	1.19	1.21
Base moment	J3x	0.38	0.20	0.96	0.96	0.33	0.22	0.98	1.28
	J3y	1.1	1.03	1.07	0.71	1.09	1.01	1.06	1.05
Deck moment	J4x	0.51	0.29	0.94	2.21	0.53	0.33	0.93	1.94
	J4y	1.33	0.97	1.51	1.01	1.32	0.96	1.52	1.79
Cable tension	J5	1.17	1.18	1.18	1.18	1.17	1.18	1.18	1.18
Longest cables tension	J5L	0.87	1.00	0.88	1.26	0.94	0.99	0.80	1.79
Deck displacement	J6	1.74	1.08	4.18	9.90	1.88	0.94	4.17	8.62

Table 2. Arrangement 2

Seismic records	Evaluation criteria	Passive				Semiactive			
		ElC	Mex	Geb	0.3 Geb	ElC	Mex	Geb	0.3 Geb
Base shear	J1x	0.31	0.20	0.43	0.52	0.31	0.22	0.42	0.43
	J1y	0.75	0.82	0.67	0.76	0.79	0.73	0.59	0.72
Deck shear	J2x	0.59	0.55	1.97	2.43	0.56	0.54	2.09	2.18
	J2y	1.28	0.78	1.10	1.04	1.27	0.76	1.09	1.11
Base moment	J3x	0.37	0.19	0.81	0.96	0.35	0.21	0.74	0.77
	J3y	0.82	0.86	0.67	0.71	0.86	0.73	0.59	0.7
Deck moment	J4x	0.72	0.27	1.85	2.21	0.63	0.32	1.88	1.6
	J4y	1.06	0.78	1.11	1.01	1.07	0.76	1.14	1.12
Cable tension	J5	1.18	1.18	1.18	1.18	1.18	1.18	1.18	1.18
Longest cables tension	J5L	0.76	0.98	1.31	1.26	0.71	0.76	1.35	1.19
Deck displacement	J6	2.95	0.83	7.69	9.90	2.58	0.83	8.01	7.19
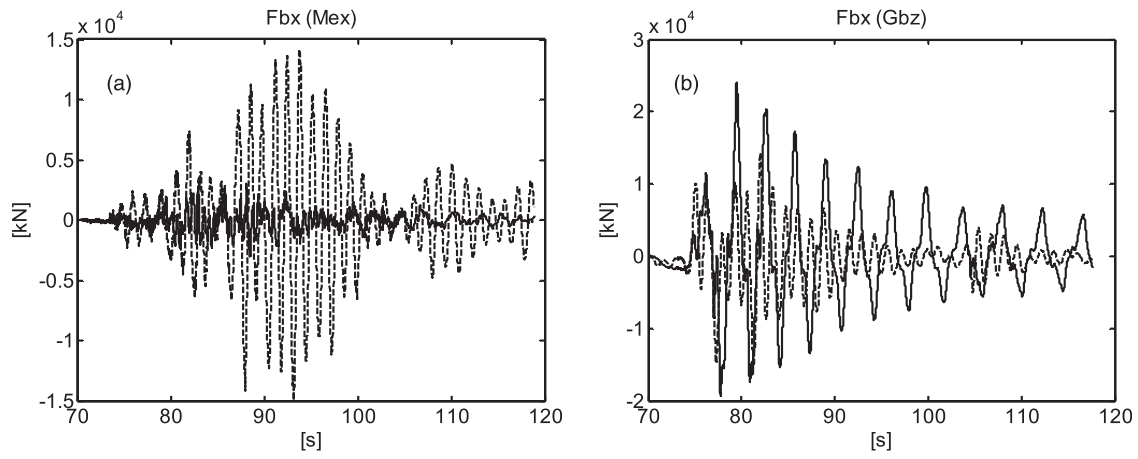
Fig. 5. Passive Arrangement 1; Pier 2 base shear in the longitudinal direction in one of the legs: (a) Mexico; (b) Gebze; dashed line: uncontrolled; first 70 s are the time stretch during which the application of the dead load and the cables pretension is carried out, and accordingly, the seismic action starts at $t = 70$ s
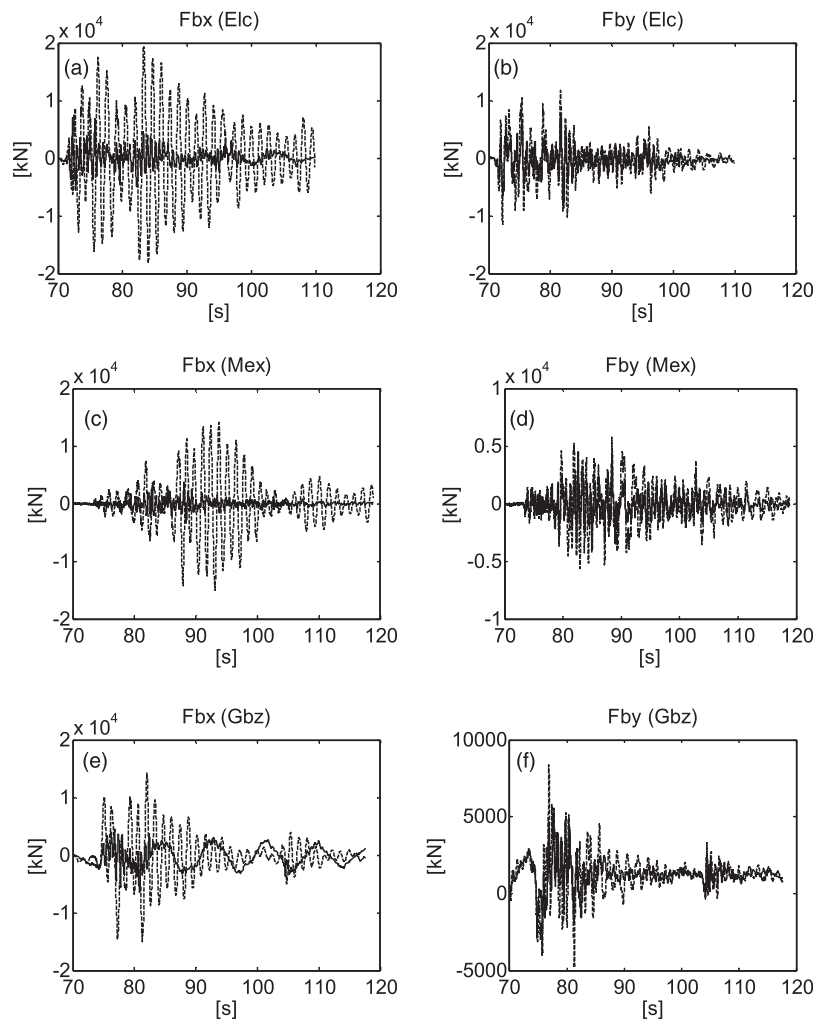
Fig. 6. Semiactive Arrangement 2; Pier 2 base shear in one of the legs: left side, longitudinal; right side, transversal; (a) and (b) El Centro; (c) and (d) Mexico; (e) and (f) Gebze; dashed line: uncontrolled; solid line: controlled

For the control Arrangements 1 and 2, these are pier base shear in the bridge x longitudinal and y transversal direction, J1; pier deck level shear in the bridge x longitudinal and y transversal direction, J2; pier base bending moment acting in the x,z- and y,z-plane, J3; pier deck level bending moment acting in the x,z- and y,z-plane, J4; cable tension, J5, also with cable tension for the longest cables only, J5L; and deck displacement along the bridge x longitudinal direction, J6. Such evaluation criteria represent the extremes of the dynamic response of the bridge and have been selected for the evaluation of the seismic control efficacy.

It is worth noticing that the internal forces at the towers' base in cable-stayed bridges result as the most onerous for the piers (Calvi et al. 2010) for both longitudinal and transversal deck motions. This descends either by the presence of shock-absorbers links or control devices, typically at the level of the deck. Fig. 4 schematically depicts this for the uncontrolled Bill Emerson bridge version.

Table 1 reports the main results in terms of evaluation criteria for Arrangement 1 for both the passive and semiactive control configurations. For evaluating the larger effectiveness of the semiactive solution with respect to the passive one, results of the Gebze record, rescaled by reducing its original strength by 30%, are shown as well. Table 2 is devoted to Arrangement 2.

Focusing attention to the passive controlled configuration of the bridge in Table 1, results for the proposed updated bridge model are

generally similar to those obtained with the model given by the original benchmark, with the same values of the device's operational parameters and the same control scheme reported by Domaneschi (2010), particularly under the El Centro (ElC) and Mexico (Mex) excitations. Under the Gebze (Geb) record, however, the internal forces and displacements are generally higher. The main reason for this consists of a resonant reaction activated by the low frequency content characterizing the Gebze record [Figs. 2 and 5(b) at around 0.1–0.3 Hz]. The incremented cable tensions reflect the improvements adopted in the simulation of the coupled deck-cable dynamics. When the semiactive scheme is implemented, equal outcomes are obtained, whereas the transversal performances are still unsatisfactory as a consequence of having implemented the original benchmark kinematic for the deck-tower relative displacements in Arrangement 1.

Figs. 5(a and b) depict the time history responses for the shear in longitudinal direction in the element of one leg at the base of Pier 2 for the passive Arrangement 1. Fig. 5(a) is devoted to the Mexico record, and highlights the positive performance of the passive system. Fig. 5(b) shows the large amplification of the controlled response induced by the resonant frequency content of the Gebze record.

In Table 1, the main results for Arrangement 1 and also when the Gebze record is rescaled and reduced to 30% of its original strength
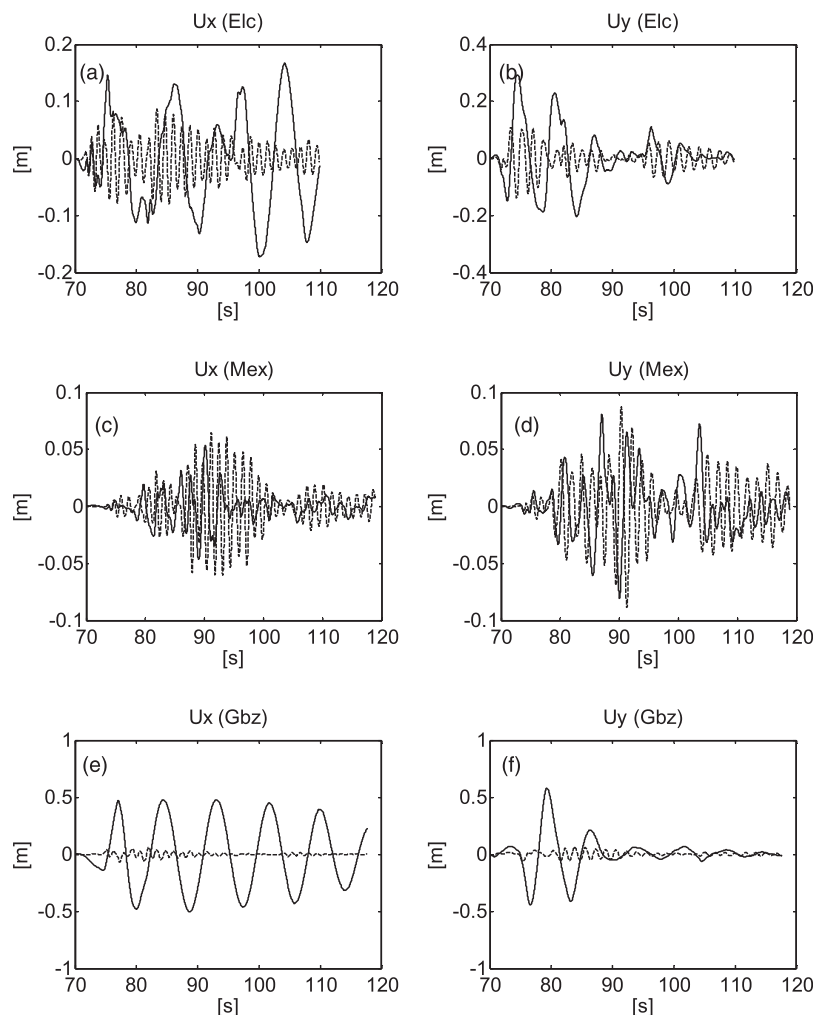
Fig. 7. Semiactive Arrangement 2; middeck displacements: left side, longitudinal; right side, transversal; (a) and (b) El Centro; (c) and (d) Mexico; (e) and (f) Gebze; dashed line: uncontrolled; solid line: controlled

(column 0.3 Geb) for evaluating the better effectiveness of the semiactive solution with respect to the passive one are reported. The resulting accelerograms have been applied to the updated bridge model in the uncontrolled and controlled configurations. Interestingly enough, the combined effects of SSI and modeling of the cables lead to performances of the control strategies that seem less effective than they proved to be on the original benchmark bridge model in the study by Domaneschi (2010). This outcome helps in assessing the significance and limits of the results obtained with the original benchmark bridge model.

Moving onto the device distribution of Arrangement 2 (Table 2), which besides SSI and enhanced cable modeling has devices applied in both the longitudinal and transversal direction and a kinematic scheme that allows the transversal motion of the deck with respect to the piers, it is first noted that the passive controlled solution is effective in both horizontal directions. In contrast to most of the literature, significantly marked positive effects of the transversal devices can be recognized, thus enhancing the knowledge base of the Bill Emerson bridge benchmark. In particular, the transversal internal forces at the pier base (criteria J1y and J3y) result effectively decreased for the first time to the authors' knowledge. The tension in the cables (criteria J5), which increases with respect to the original statement (Domaneschi 2010), remains in an acceptable range. In particular, the control system mitigates the tension in the longest cables (criteria J5L) for the El Centro and Mexico record, whereas the response increases for the resonance reasons already pointed out for Arrangement 1 for the Gebze record.

The semiactive control strategy leads to outcomes in-line with those of the passive one, with the notable exception that the control solution is now able to adapt itself to the new seismic intensity, showing a reasonable better efficiency when the input is scaled (Table 2). Fig. 6 depicts the base shear in one leg of Pier 2 for the nominal intensity of the considered seismic records, highlighting the positive performance of both longitudinal and transversal semiactive devices and the predominant efficacy of the longitudinal ones. The displacements at middeck (Fig. 7) show the expected increments that are typical of the implementation of passive and semiactive control strategies, with respect to the uncontrolled configuration, with rigid link and shock absorbers as deck-tower connections.

A summary of the role and effects related to the different arrangements of the devices envisaged herein can be gained by looking at the devices' hysteresis cycles. Fig. 8(a) shows the ones for the El Centro record of the passive control device at Pier 2 in Arrangement 1, whereas Figs. 8(b and c) show those in Arrangement 2 at the same location. The inclined stay cables transmit the longitudinal motion of the foundations from the vertical structure to the deck, which in the longitudinal direction, performs a marked rigid body motion relative displacement with respect to the piers. When the rigid transversal links are removed and the bridge deck experiences bidirectional movements (Arrangement 2), the longitudinal devices undergo a smaller stroke while the driving effect of the pier on the transversal deck motion is achieved at a lesser extent due to the quasi-vertical shape of the stay cables. The different dissipations in the hysteresis cycles depicted in Fig. 8(b) highlights this difference. Such behavior is less evident after implementing the semiactive control scheme [Fig. 8(c)] when the yielding limit is reduced. In light of these observations, it is worth noting how remarkable the positive contribution of the structural control devices is, despite the small relative displacements of the nodes where they are connected.

From the point of view of the dynamical structural response, because the analyses were carried out in large displacements, there is a natural coupling between the transversal motion of the deck and the longitudinal response of the structure. The deck lateral displacements are larger. By examining the loci of the midspan position
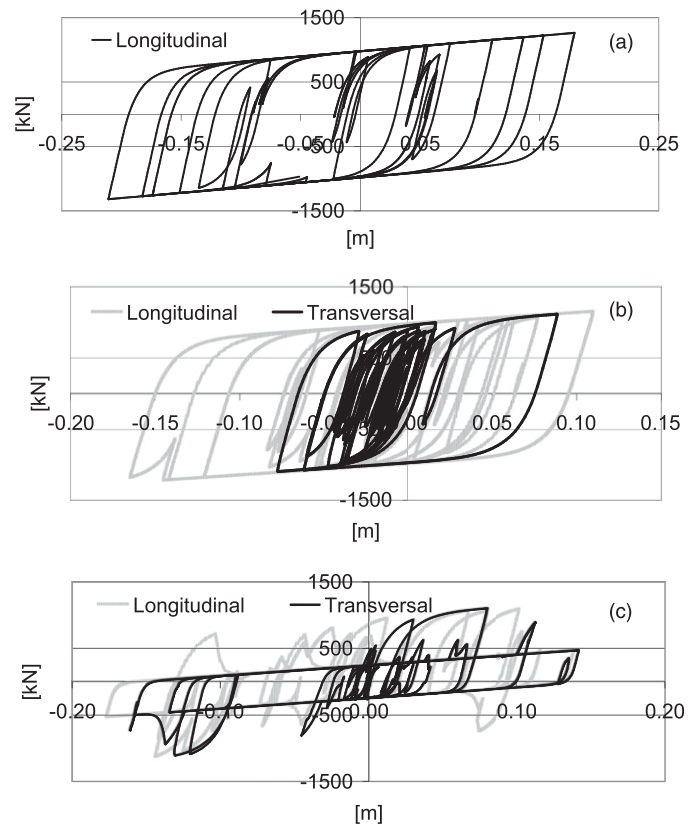
Fig. 8. Hysteresis cycles for El Centro at Pier 2: (a) Arrangement 1 passive devices; (b) Arrangement 2 passive; (c) semiactive ones

during the three earthquake signals considered here, an appreciable correlation for only the Gebze signal in the controlled configuration was found.

Conclusions

In this paper, the second-generation ASCE benchmark control problem is considered by implementing SSI and improved cable modeling. Passive and decentralized semiactive control strategies are proposed to reduce the earthquake-induced forces in a cable-stayed bridge. An independent numerical model of the bridge is developed, and two different arrangements of the control devices are considered. Arrangement 1 is equivalent to the original benchmark and does not allow the transversal relative motion of the deck with respect to the piers. Such a choice results in ineffective control and unsatisfactory values of the evaluation criteria when SSI and refined cable modeling are adopted. Arrangement 2 substantially differs in the adopted static scheme because it lacks the transversal rigid links and adopts control devices working in both horizontal directions. Arrangement 2 clearly improves the structural response and sports a good outcome from the evaluation criteria.

The numerical simulation results demonstrate that the performance of the proposed semiactive control design, implementing the on/off sky-hook algorithm, is able to perform as efficiently as the passive scheme for all the earthquake signals of the original benchmark and to adapt itself when the seismic intensity is scaled, showing an equivalent level of protection. This result comes at the cost of slightly higher deck relative displacements. The differences between the results obtained in the new framework and the ones from the literature can be mainly traced to the major kinematical improvements introduced in the bridge model. Cable dynamics

significantly affect the cable tension and deck displacements in the controlled configuration. Shear forces and bending moments at the base of the tower are significantly affected as well.

Acknowledgments

References

ANSYS. (2011). *Academic release 12 user manual*, ANSYS, Canonsburg, PA.

Caetano, E., Cunha, A., Gattulli, V., and Lepidi, M. (2008). "Cable-deck dynamic interactions at the International Guadiana Bridge: On-site measurements and finite element modelling." *Struct. Control Health Monit.*, 15(3), 237–264.

Caicedo, J. M., Dyke, S. J., Moon, S. J., Bergman, L. A., Turan, G., and Hague, S. (2003). "Phase II benchmark control problem for seismic response of cable-stayed bridges." *J. Struct. Control*, 10(3–4), 137–168.

Calvi, G. M., Sullivan, T. J., and Villani, A. (2010). "Conceptual seismic design of cable-stayed bridges." *J. Earthquake Eng.*, 14(8), 1139–1171.

Casciati, F., and Faravelli, L. (1991). *Fragility analysis of complex structural systems*, Taunton, Somerset, U.K.

Casciati, F., Magonette, G., and Marazzi, F. (2006). *Technology of semi-active devices and applications in vibration mitigation*, Wiley, West Sussex, U.K.

Chen, W. F., and Duan, L. (2000). *Bridge engineering handbook*, CRC, Boca Raton, FL.

Clough, R. W., and Penzien, J. (1975). *Dynamics of structures*, McGraw Hill, New York.

Domaneschi, M. (2010). "Feasible control solutions of the ASCE benchmark cable-stayed bridge." *Struct. Control Health Monit.*, 17(6), 675–693.

Domaneschi, M. (2012). "Simulation of controlled hysteresis by the semi-active Bouc-Wen model." *Comput. Struct.*, 106–107, 245–257.

Domaneschi, M., and Martinelli, L. (2012). "Performance comparison of passive control schemes for the numerically improved ASCE cable-stayed bridge model." *Earthquake Struct.*, 3(2), 181–201.

Domaneschi, M., Martinelli, L., and Romano, M. (2010). "A strategy for modelling external user element in ANSYS: The Bouc-Wen and the Skyhook case." *Proc., 34th IABSE Symp.*, International Association for Bridge and Structural Engineering, Zurich, Switzerland.

Dyke, S. J., Caicedo, J. M., Turan, G., Bergman, L. A., and Hague, S. (2003). "Phase I benchmark control problem for seismic response of cable-stayed bridges." *J. Struct. Eng.*, 10.1061/(ASCE)0733-9445(2003)129:7(857), 857–872.

Fallah, A. Y., and Taghikhany, T. (2011). "Time-delayed decentralized H_2/LQG controller for cable-stayed bridge under seismic loading." *Struct. Control Health Monit.*, 20(3), 354–372.

Frangopol, D. M., Saydama, D., and Kima, S. (2012). "Maintenance, management, life-cycle design and performance of structures and infrastructures: A brief review." *Struct. Infrastruct. Eng.*, 8(1), 1–25.

Gattulli, V., and Lepidi, M. (2007). "Localization and veering in the dynamics of cable-stayed bridges." *Comput. Struct.*, 85(21–22), 1661–1678.

He, W.-L., and Agrawal, A. K. (2007). "Passive and hybrid control systems for seismic protection of a benchmark cable-stayed bridge." *Struct. Control Health Monit.*, 14(1), 1–26.

Ikeda, Y. (2009). "Active and semi-active vibration control of buildings in Japan—Practical applications and verification." *Struct. Control Health Monit.*, 16(7–8), 703–723.

Ismail, M., Rodellar, J., Carusone, G., Domaneschi, M., and Martinelli, L. (2013). "Characterization, modeling and assessment of Roll-N-Cage isolator using the cable-stayed bridge benchmark." *Acta Mech.*, 224(3), 525–547.

Kelly, J. M. (2004). "Seismic isolation." Chapter 11, *Earthquake engineering from engineering seismology to performance based design*, Y. Bozorgnia and V. Bertero, eds., CRC, Boca Raton, FL.

Loh, C.-H., and Chang, C.-M. (2006). "Vibration control assessment of ASCE benchmark model of cable-stayed bridge." *Struct. Control Health Monit.*, 13(4), 825–848.

Martinelli, L., Barbella, G., and Feriani, A. (2010). "Modeling of Qiandao Lake submerged floating tunnel subject to multi-support seismic input." *Procedia Eng.*, 4, 311–318.

Martinelli, L., Barbella, G., and Feriani, A. (2011). "A numerical procedure for simulating the multi-support seismic response of submerged floating tunnels anchored by cables." *Eng. Struct.*, 33(10), 2850–2860.

MATLAB [Computer software]. Natick, MA, MathWorks.

Park, K.-S., Jung, H.-J., Spencer, B. F., Jr., and Lee, I.-W. (2003). "Hybrid control systems for seismic protection of a phase II benchmark cable-stayed bridge." *J. Struct. Contr.*, 10(3–4), 231–247.

Podolny, W., Jr. (1980). "Cable-stayed bridges: A current review." *Ann. N. Y. Acad. Sci.*, 352, 71–85.

Preumont, A. (2002). *Vibration control of active structures*, Springer, Berlin.

Sieffert, J. G., and Cevaer, F. (1992). *Handbook of impedance function*, Presses Academiques, Editions Ouest, Nantes, France.

Spencer, B. F., Jr., and Nagarajaiah, S. (2003). "State of the art of structural control." *J. Struct. Eng.*, 10.1061/(ASCE)0733-9445(2003)129:7(845), 845–856.

University Transportation Center at the University of Missouri-Rolla (UTC-UMR). (2007). "Assessment of the Bill Emerson Memorial Cable-Stayed Bridge based on seismic instrumentation data." *Organizational Results Research Rep. No. OR08.003*. ⟨http://library.modot.mo.gov/RDT/reports ../Ri05023/or08003.pdf⟩ (Nov. 14, 2013).

Wilson, J. C., and Gravelle, W. (1991). "Modelling of a cable-stayed bridge for dynamic analysis." *Earthquake Eng. Struct. Dyn.*, 20(8), 707–721.